# Model of Signal In Space Biases in the Integrity Support Message and Advanced RAIM Algorithm

Ilaria Martini*, Boubeker Belabbas*, Santiago Perea* and Michael Meurer*†
*German Aerospace Center (DLR), Munich, Germany
†Chair of Navigation, RWTH Aachen University, Germany

## BIOGRAPHIES

**Dr. Ilaria Martini** received the Master Degree in telecommunication engineering and the Ph.D. in information technology from the University of Florence, Italy. She was at the Galileo Project Office of ESA/ESTEC in 2003, working on the performance of the Galileo Integrity Processing Facility. She was research associate in 2004 at the University of Florence and in 2005 at the the Federal Armed Forces Germany in Munich. In 2006 she joined the navigation department of Ifen GmbH in Munich. Since 2012 she works as research associate in the Institute of Communication and Navigation at the German Aerospace Center (DLR), Oberpfaffenhofen. Her main area of interest is GNSS Integrity Monitoring.

**Boubeker Belabbas** obtained a MSc. Degree in Mechanical Engineering from ENSEM in Nancy (France) and a specialized MSc. Degree in Aerospace Mechanics from SUPAERO in Toulouse (France). He joined DLR in 2001 and developed the navigation integrity activities. He now leads the GNSS integrity team within the Department of Navigation at the Institute of Communications and Navigation. His field of competence includes GNSS with augmentations (SBAS, GBAS), Advanced Receiver Autonomous Integrity Monitoring, GNSS/INS Hybridization with integrity, and Alternative Positioning Navigation and Timing.

**Santiago Perea** obtained a Master of Science in Aerospace Engineering from University of Sevilla (Spain) in 2013. In parallel, as a double degree student, he gained his Master in Mechanical and Aerospace Engineering from Illinois Institute of Technology (IIT) in 2013. Currently he is part of the staff at the Institute of Communications and Navigation at German Aerospace Center (DLR). His research focuses on Integrity Support Message (ISM) design for Receiver Autonomous Integrity Monitoring (RAIM).

**Dr. Michael Meurer** received the diploma in electrical engineering and the PhD degree from the University of Kaiserslautern, Germany. After graduation, he joined the Research Group for Radio Communications at the Technical University of Kaiserslautern, Germany, as a senior key researcher, where he was involved in various international and national projects in the field of communications and navigation both as project coordinator and as technical contributor. From 2003 till 2013, Dr. Meurer was active as a senior lecturer and Associate Professor (PD) at the same university. Since 2006 Dr. Meurer is with the German Aerospace Centre (DLR), Institute of Communications and Navigation, where he is the director of the Department of Navigation and of the center of excellence for satellite navigation. In addition, since 2013 he is a professor of electrical engineering and director of the Institute of Navigation at the RWTH Aachen University. His current research interests include GNSS signals, GNSS receivers, interference and spoofing mitigation and navigation for safety-critical applications.

## ABSTRACT

This paper focuses on the model of the Signal In Space biases in the Integrity Support Message (ISM) and Advanced RAIM (ARAIM) user algorithm. Signal distortions, satellite orbit and clock missmodelling, antenna phase center offsets, inter-frequency biases and other satellite related errors generate biases in the ranging error distributions which must be included in the error model and handled in the integrity algorithm.
The scope of this paper is to investigate the design of these biases in the ISM in order to optimize the user availability and integrity performance.
The study of present ARAIM algorithms shows situations where the conservatism of the biases model can degrade significantly the user availability. One of the reason is related to the assumption that the signs of these biases are unknown. An investigation on the methodology to handle the signs is provided. An improved approach is presented using this information and modelling it in both ISM and ARAIM algorithm. This approach allows to improve the user availability and integrity performance by reducing the protection levels. The user performance improvement was

confirmed during an experimentation activity performed with service volume simulations. Finally the performance improvement was confirmed with an analysis on real data collected during a GPS-Galileo dual frequency flight campaign performed in March 2015.

## INTRODUCTION

In the rapidly evolving GNSS scenario it is important to properly model each user ranging error component. Those which were considered in the past of minor importance for single frequency users represent today the major performance drivers for multiconstellation dual frequency users and need to be properly taken into account.

These errors, so called Signal In Space Errors, are caused by satellite orbit and clock navigation message mismodelling, signal distortions, antenna phase center offsets, inter-frequency biases and code carrier incoherence. It is intrinsically difficult to model and correct these errors, because they are dependent on the receiver and the satellite characteristics [2], [3], [4], [5]. Their variations cannot be a priori estimated and consequently generate residual errors. For this reason the statistic model used for these Signal In Space error includes biases. The Integrity Support Message foreseen in the ARAIM concept models these biases in the so called $b_{nom}$ [1].

Present ARAIM user algorithms assume that the signs of these biases are unknowns [1], [6], [7]. The reason for that is related to the variation of these biases with the receiver hardware configuration, the satellite processing chain and the ground estimation method. Besides the projection of the same bias into the visibility area has different signs at different user locations. The consequence is that the biases $b_{nom}$ are set positive for each satellite and the user estimates its bias in the position domain considering their worst case projection. This conservative approach leads to increased protection levels and reduced user availability.

Another undesired effect of this approach is the inflation of protection levels in cases where the corresponding position error is actually not affected by these biases. In particular combination of satellite biases leading to position biases only in the vertical (horizontal) direction generate biases in the ARAIM horizontal (vertical) protection levels. This also happens with biases common to all satellites, which are absorbed in the user clock and do not affect the user position accuracy. These harmless biases generate inflated protection levels and consequently degrade user availability.

This paper aims to investigate this aspect from an analytical point of view, with a study of the impact of satellite biases on the user positioning and integrity performance. ARAIM protection level and fault detection algorithm are analyzed with a particular focus on the effect of the assumption of unknown bias signs.

The second part of the paper presents an ISM bias model where the information on the bias signs is included in the ISM. The modifications to the ARAIM user algorithms [1] to take advantage of the additional information are described. Finally the paper shows the improvement in terms of availability and integrity performance with simulated data and with real data collected during a dual frequency GPS-Galileo flight campaign performed in March 2015.

## 1 IMPACT OF SIGNAL IN SPACE BIASES ON USER POSITIONING

The measurement model of the user positioning algorithm [1], [6] is based on the following equation:

$$\boldsymbol{\rho} = \boldsymbol{G}\boldsymbol{x} + \boldsymbol{\varepsilon} + \boldsymbol{b}^{Sat} \tag{1}$$

where

- $\boldsymbol{x}$ is the $(3 + N_{const}) \times 1$ vector with the user position offset in the local reference frame (east, north, up), the user clock offset and the inter-constellation time offsets,
- $N_{const}$ is the number of constellations used
- $\boldsymbol{\rho}$ is the $N_{sat} \times 1$ vector with the pseudorange measurements minus the expected ranging values,
- $N_{sat}$ is the number of satellites used,
- $\boldsymbol{G}$ is the $N_{sat} \times (3 + N_{const})$ geometry matrix as defined in [1], [6],
- $\boldsymbol{\varepsilon}$ is the $N_{sat} \times 1$ vector with the pseudorange measurements noise. Each component of $\boldsymbol{\varepsilon}$ follows an unbiased gaussian distribution,
- $\boldsymbol{b}^{Sat}$ is the $N_{sat} \times 1$ vector of residual ranging biases.

The position solution obtained by means of a weighted least-squares estimation is

$$\boldsymbol{x} = \boldsymbol{S}\boldsymbol{\rho} \tag{2}$$

where

- $\boldsymbol{S} = (\boldsymbol{G}^T\boldsymbol{C}^{-1}\boldsymbol{G})^{-1}\boldsymbol{G}^T\boldsymbol{C}^{-1}$ is the $(3+N_{const}) \times N_{sat}$ pseudoinverse matrix
- $\boldsymbol{C}$ is the covariance matrix of the pseudorange noise.

The biases affecting the user position solution are

$$b_q^{User,True} = \sum_{i=1}^{N_{sat}} \boldsymbol{S}_{q,i} b_i^{Sat} \tag{3}$$

where $q = 1, 2$ correspond to the horizontal components and $q = 3$ to the vertical one.
A special case is represented by bias combinations, $\boldsymbol{b}^{Sat}$, which affect only one component of the user position error, $\boldsymbol{b}^{User,True}$. These vectors belong to the space generated by one column of the geometry matrix. They are also orthogonal to the parity space and likely undetectable by ARAIM fault detection and exclusion algorithm. They can be expressed as

$$\boldsymbol{b}^{Sat} = k\boldsymbol{G}\boldsymbol{e}_j \tag{4}$$

where $k \in \Re$ and $\boldsymbol{e}_j$ is the $j^{th}$ column of the $N_{sat} \times N_{sat}$ identity matrix.
These biases affect only one user position component: the $j^{th}$ one. In fact

$$\begin{aligned} \boldsymbol{b}^{User,True} &= (\boldsymbol{G}^T\boldsymbol{C}^{-1}\boldsymbol{G})^{-1}\boldsymbol{G}^T\boldsymbol{C}^{-1}k\boldsymbol{G}\boldsymbol{e}_j \\ &= k(\boldsymbol{G}^T\boldsymbol{C}^{-1}\boldsymbol{G})^{-1}\boldsymbol{G}^T\boldsymbol{C}^{-1}\boldsymbol{G}\boldsymbol{e}_j \\ &= k\boldsymbol{e}_j \end{aligned} \tag{5}$$

Any combination of range measurement biases resulting in a vector parallel to the $j^{th}$ column of the design matrix generates a bias in the user position solution which exclusively affects the specific $j^{th}$ component. The case of bias common to all the satellites is a particular case of this condition. These cases represent specific conditions of the ARAIM algorithm, where its conservatism produces the worst effects. In the following section the ARAIM algorithm performance in these cases will be analyzed and described.

## IMPACT OF SIGNAL IN SPACE BIASES ON USER INTEGRITY

As previously described, ARAIM protection level and fault detection algorithms [1] are based on the assumption that the signs of the nominal biases are not known to the user and the absolute value of each nominal bias is bounded by $\boldsymbol{b}_{nom}$ listed in the ISM.
The ISM contains the parameters listed in Table 1 as specified in [1].
The satellite ranging bias is modelled with only one parameter, $\boldsymbol{b}_{nom}$. The bias vector containing $b_{nom}$ of all the satellites is projected in the user position domain considering the worst case projection. This occurs when the nominal bias of each measurement has the same sign of the coefficient projecting the pseudorange onto the position.
The biases used in the ARAIM algorithm [1] are then

$$b_q^{User,ARAIM} = \sum_{i=1}^{N_{sat}} |\boldsymbol{S}|_{q,i} b_{nom,i} \tag{6}$$

For this bias the property described by equation 5 is not valid anymore. The consequence is that biases affecting only one component in the position domain lead to inflation of protection level of unbiased components. In addition, also common biases degrade the user availability and continuity by increasing both the vertical and horizontal protection levels.
The following sections show the details of the user performance in these specific worst cases.

**Table 1** ISM content

| ISM paramter | Description | Number of bits |
|---|---|---|
| $Mask_i$ | 32 bits indicating whether a satellite is valid for ARAIM (1) or not (0) | 32 bits |
| $P_{const,i}$ | Probability of constellation fault at a given time | 2 bits |
| $P_{sat,j}$ | Probability of satellite fault at a given time | 2 bits |
| $\alpha_{URA,j}$ | Multiplier of the URA/SISA for integrity | 3 bits |
| $\alpha_{URE,j}$ | Multiplier of the URA/SISA for continuity and accuracy | 3 bits |
| $b_{nom,j}$ | Nominal bias term in meters | 4 bits |

### 1.1 Ranging Common Bias

The consequence of the ARAIM approach on the user performance and its degradation have been analyzed and quantified by means of simulations. For this purpouse the inflation factor of the biases operated by the ARAIM worst case projection is defined as follows

$$k_q^{Inflation} = \frac{|b_q^{User,ARAIM}|}{|\boldsymbol{b}^{User,True}|} \tag{7}$$

This factor shows the conservatism of the ARAIM approach when using equation 6 to model the bias described in equation 3. An inflation factor close to 1 indicates no performance degradation. As the inflation factor increases, the user performance degrade.
Figure 1 shows this inflation factor in a 24 hours simulation of GPS+Galileo constellation. A user grid of 5x5 degree has been used and a common bias of 1m has been added to the nominal ranging error. This bias is completely absorbed in the user clock offset, but generates protection level biases. In this result and in the following ones, it is assumed that the ISM $b_{nom}$ contains the accurate value of $\boldsymbol{b}^{Sat}$ without estimation error. Figure 1 shows the fourth component of the inflation factor, $k_4^{Inflation}$, as function of the user location.

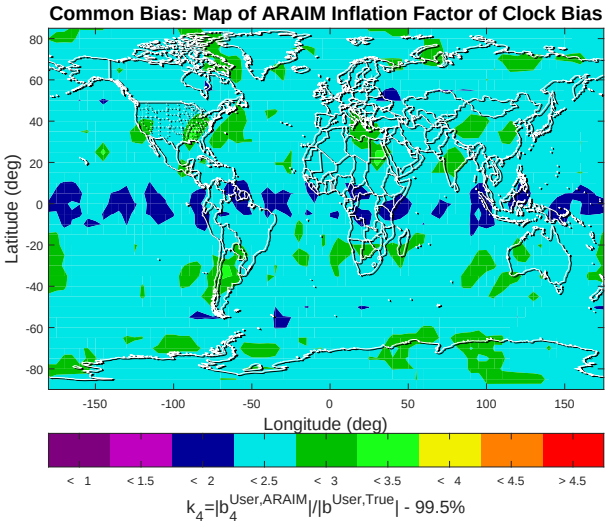


**Fig. 1** Simulation of Common Range Bias: map of the inflation factor of the user clock offset estimated by ARAIM when considering the worst case projection

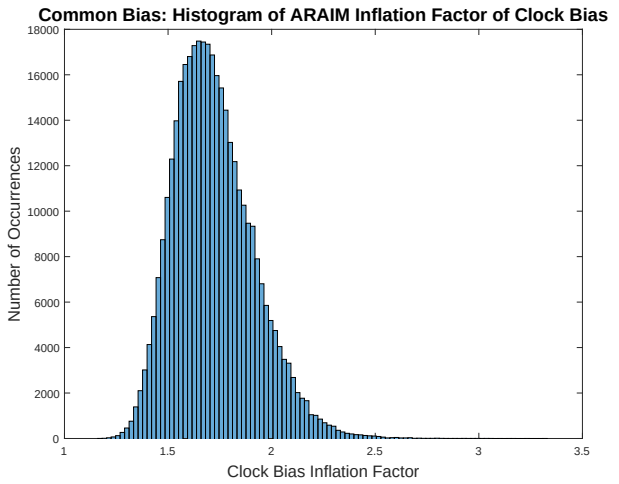


**Fig. 2** Simulation of Common Range Bias: histogram of the inflation factor of the user clock offset estimated by ARAIM when considering the worst case projection

Although this bias component doesn't affect the user and is not used in the user integrity algorithm, it is interesting to observe how significant its inflation can be. The map in Figure 1 shows situation where this inflation can be bigger than 3.5. The histogram in Figure 2 shows the distribution of the clock bias inflation factor, $k_4^{Inflation}$.
When a common bias is present not only the clock bias is inflated, but also the vertical and horizontal ARAIM biases are different from zero, as shown in Figure 3 and 4 displaying the vertical bias inflation factor, $k_3^{Inflation}$, as function of the user location and its histogram:

$$k_3^{Inflation} = \frac{\left| b_3^{User,ARAIM} \right|}{\left| \boldsymbol{b}^{User,True} \right|} \tag{8}$$

In this case the vertical protection level are biased although the actual ranging errors are unaffected. The results show an inflation factor equal to 2.5 in average and it can be bigger than 4.
The horizontal bias,

$$\boldsymbol{k}_{1,2}^{Inflation} = \sqrt{\left(k_1^{Inflation}\right)^2 + \left(k_2^{Inflation}\right)^2} \tag{9}$$

presents the same behaviour as shown in Figure 5 and 6.

### 1.2 Biases Affecting Only One Position Component

This section analyses the case of SIS bias combinations affecting one position error component. This case is investigated to show that there are situation of bias-free ranging error resulting in biased protection levels: ranging biases resulting in only horizontal (vertical) biases at user level generate also biases in the vertical (horizontal) protection level.

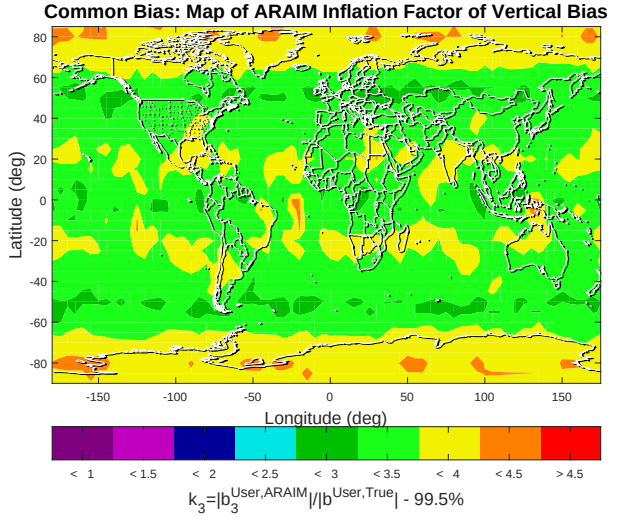


**Fig. 3** Simulation of Common Range Bias: map of the inflation factor of the user vertical bias estimated by ARAIM when considering the worst case projection

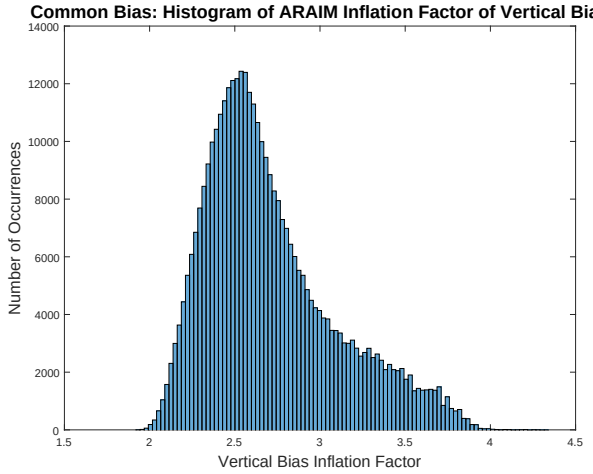


**Fig. 4** Simulation of Common Range Bias: histogram of the inflation factor of the user vertical bias estimated by ARAIM when considering the worst case projection

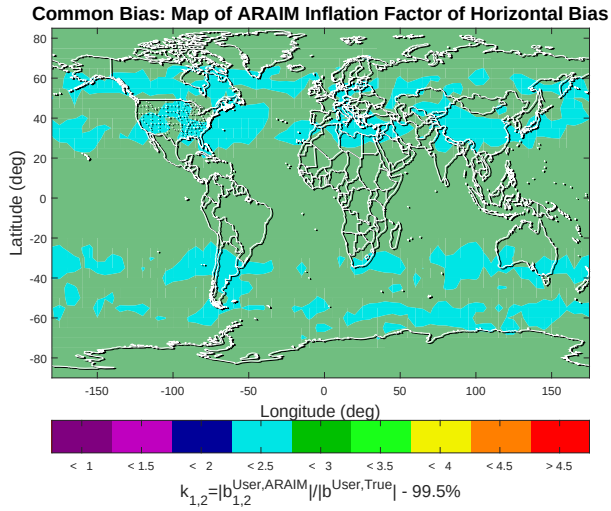


**Fig. 5** Simulation of Common Range Bias: map of the inflation factor of the user horizontal bias estimated by ARAIM when considering the worst case projection

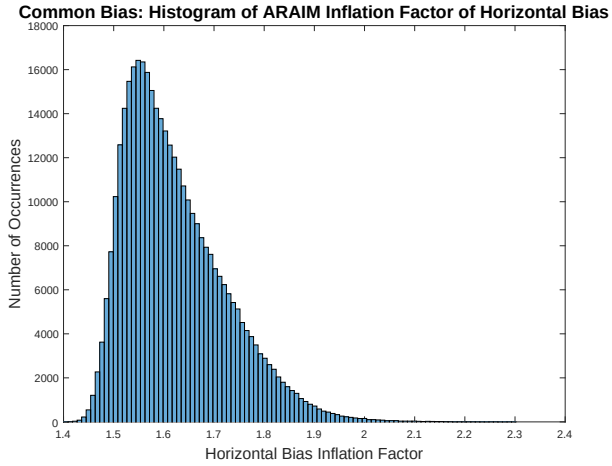


**Fig. 6** Simulation of Common Range Bias: histogram of the inflation factor of the user horizontal bias estimated by ARAIM when considering the worst case projection

Figure 7 and 8 show the worst case vertical bias in case of true bias combinations affecting only the horizontal position. This result has been obtained with a 24 hours simulation of GPS+Galileo dual frequency user worldwide with a 5x5 degree user grid. Each epoch the bias corresponding to the sum of the first two columns of the geometry matrix (expressed in local reference system east, north, up) has been added to the ranging error vector:

$$\boldsymbol{b}^{Sat} = \boldsymbol{G}(\boldsymbol{e}_1 + \boldsymbol{e}_2) \tag{10}$$

The results shows the vertical component of the inflation factor, $k_3^{Inflation}$.
The same is valid for biases affecting only the vertical position component shown in Figure 9 and 11 showing the horizontal inflation factor, $k_{1,2}^{Inflation}$, when the ranging bias used is

$$\boldsymbol{b}^{Sat} = \boldsymbol{G}\boldsymbol{e}_3 \tag{11}$$

Also in these cases the user position error presents biases in components which should be not affected and should be bias-free. Besides these biases are even amplified in the horizontal direction with an average inflation factor of 1.2 and in the vertical one with an average factor of 1.5.

## 2 SIS BIAS MODEL OPTIMIZING THE AVAILABILITY PERFORMANCE

A possible solution to reduce the effect described in the previous sections is removing the component of the ranging biases common to all the satellites of each constellation. In this way, $b_{nom}$ models only the residual differential bias. This solution aims to address the specific issue caused by common biases, but it does not solve the problem. It effectively reduces the effect but it doesn't eliminate all the problematic cases. In fact the ranging bias affecting only

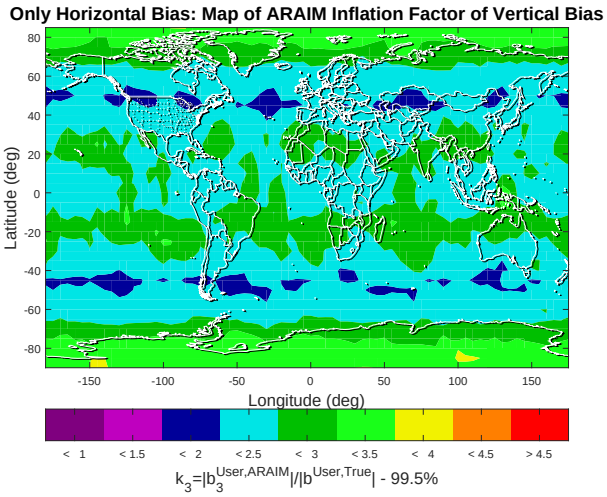


**Fig. 7** Simulation of Horizontal-only Range Bias: map of the inflation factor of the user vertical bias estimated by ARAIM when considering the worst case projection

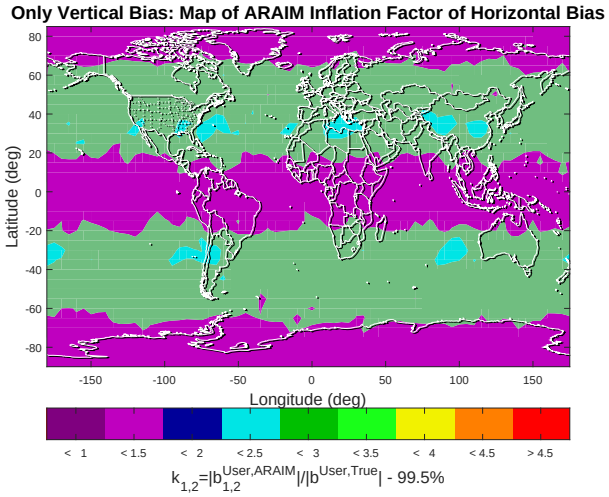


**Fig. 9** Simulation of Vertical-only Range Bias: map of the inflation factor of the user horizontal bias estimated by ARAIM when considering the worst case projection

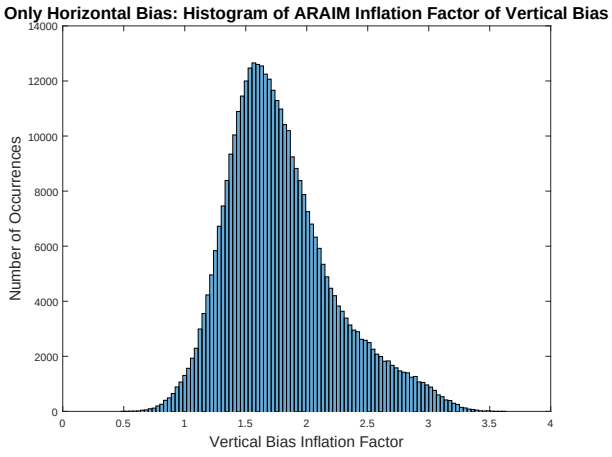


**Fig. 8** Simulation of Horizontal-only Range Bias: histogram of the inflation factor of the user vertical bias estimated by ARAIM when considering the worst case projection

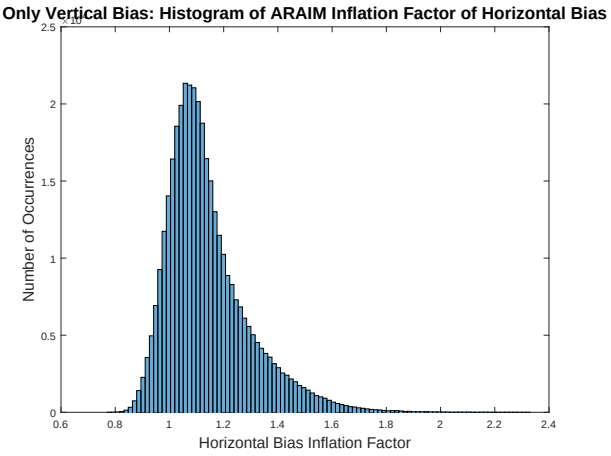


**Fig. 10** Simulation of Vertical-only Range Bias: histogram of the inflation factor of the user horizontal bias estimated by ARAIM when considering the worst case projection

the clock solution is that common only to the satellites in view and not to all.

Figure 11 shows an example where a bias is inserted which has zero mean among the satellites of one constellation. As it can be seen the VPL bias is inflated because each user observes a subset of satellites whose common bias is different from zero.

Besides this solution does not address the other cases occurring when one position error component is bias-free but the protection level is inflated.

This paper proposes an alternative approach which makes use of the ranging bias signs and aims to remove the worst case projection approach.

The Signal In Space Error contains components which depends on the satellite elevation and even on the line of sight direction. These are in particular satellite orbit error and satellite antenna offsets. They can be represented as a four dimensional vector, whose components (along-track, cross-track, radial and clock) are gaussian distributed. These error components can be estimated, each one with sign, using a network of monitoring stations [1].

The other error sources (signal distortions, code carrier coherency, inter-frequency biases) are mostly independent on the satellite elevation and are difficult to be estimated. They are assumed unknown in the present ARAIM algorithms, because they largely depends on the receiver configuration and characteristics. Actually it is possible to have their characterization for example using high gain antenna facilities, as some studies show [10], [11]. These components can be characterized as function of the receiver characteristics (correlator spacing, bandwidth, etc.) and their sign is estimated as well. This paper assumes that thanks to these characterization methods [10], [11], the variability of the biases components can be reduced by providing guideline to the receiver manufactures and by defining minimum operational performance (MOPS). It is expected that this process will evolve in the future. This would limit the variation of the biases among several receivers and would allow to identify an interval of residual biases including the signs. This scenario would allow the use of the proposed approach.

It is observed that the proposed solution addresses both the offline and the online ARAIM architecture but with a significant difference. In the online architecture the geometry dependent biases can be modelled in the ephemeris and clock corrections [1]. In this case the $b_{nom}$ would model only the error sources not depending on the geometry (signal distortions, code carrier coherency, inter-frequency biases) estimated using methods analogous to those described in [10], [11], which provide a range of biases with signs. In the offline architecture the $b_{nom}$ models also residual geometry dependent biases.

Figure 12 shows the two processing steps performed by the ARAIM algorithm when projecting the SIS error from the signal in space domain (4D vector for each satellite) to the

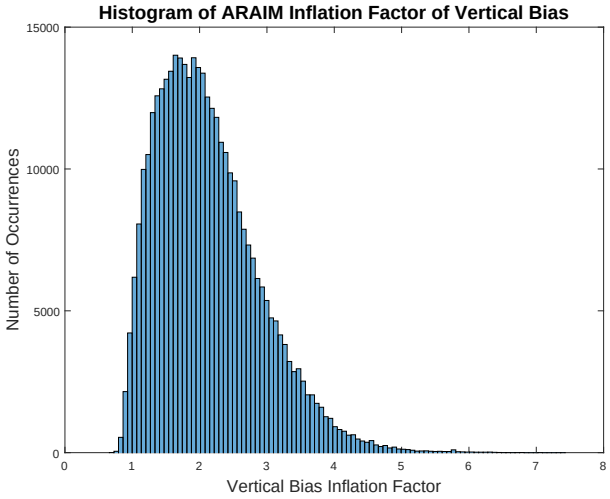


**Fig. 11** Simulation of Bias with zero mean: histogram of the inflation factor of the user vertical bias estimated by ARAIM when considering the worst case projection approach

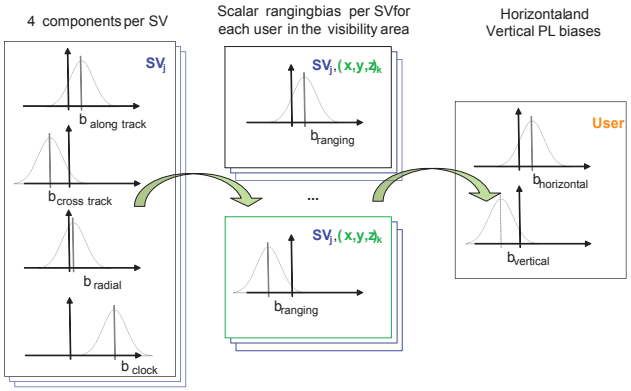


**Fig. 12** Signal In Space Projections from space domain to user domain

ranging domain (scalar value for each user in the satellite footprint) and secondly to the user position domain through the geometry matrix.
The ARAIM ground monitoring will assess the ISM parameters to be sent to the user without knowing the user specific location. The estimation process is based on satellite ranging measurements coming from a monitoring network of sensor stations. Thanks to the geometry diversity of the monitoring network it is possible to estimate and separate the 4 satellite error components (along track, cross track, radial and clock). Also the signs can be accurately estimated.
These errors must be then projected from the satellite domain to the ranging domain in particular into the ranging direction pointing to the user locations in the satellite footprint. At the present the ISM [1] uses only one parameter to model the ranging bias $b_{nom}$. The ISM information is finally used by the user to estimate its specific ranging error by projecting the biases into the position domain.
Figure 13 shows the ARAIM approach. The ISM estimation process considers the maximum absolute value of the biases and model it as $b_{nom}$.
As previously described, the best method to reduce the ARAIM conservatism is introducing the information on the biases signs in the ISM parameters.
The first possibility for realizing this is to use two parameters instead of one to model the ranging biases in the ISM: a minimum, $b_{nom,min}$, and maximum, $b_{nom,max}$, bias. These would be computed by estimating the range of variation of the biases in the satellite footprint projections and taking into account also the ground monitoring estimation accuracy. This process would result in a $\alpha$-confidence interval of the ranging bias for each satellite in the visibility area, $[b_{nom,min}, b_{nom,max}]$. It is important to note that the interval boundaries are both signed values. The following is valid for $\boldsymbol{b}^{Sat}$

$$Pr(\boldsymbol{b}^{Sat} \in [\boldsymbol{b}_{nom,min}, \boldsymbol{b}_{nom,max}]) \geq \alpha \qquad (12)$$

With these two values the user can then assess the minimum and maximum bias value in the position domain. It is noted that the minimum and the maximum position biases are generated not necessarily by the interval boundaries, $b_{nom,min}$ and $b_{nom,max}$. They can be generated by a ranging bias in between. The user has to search for the minimum and maximum biases in the position domain for all the ranging bias in the interval $[b_{nom,min}, b_{nom,max}]$. This process is illustrated in Figure 14.
It is observed that this step doesn't preserve the gaussianity property of the errors because a non-linearity is introduced in the process when the maximum bias over the satellite footprint (WUL) is selected.
Another alternative solution is to use the 4D error model and use 4 parameters in the ISM to model the SIS biases. This approach requires more bandwidth (4x4 bits instead of 4 for the bias parameters) in the ISM but has several advantages:

- the user can estimate its specific bias with sign
- the property of gaussianity of the final user position error is preserved thanks to the linearity of all the processes involved. This simplifies the ISM estimation algorithm which doesn't need to estimate the confidence interval as in the first approach (Figure 14). Thanks to the linearity the estimation accuracy can easily be included in the URA sigma value. This explains also why for each component only one parameter is needed and not a minimum and a maximum extreme of the confidence interval like in the 2 parameters case.
- this solution improves the performance of the previous approach because no worst user location approach is used.

It is important to highlight that in the online ARAIM architecture the geometry dependent biases can be modelled in the ephemeris and clock corrections. The $b_{nom}$ would include the other error components (signal distortions, code

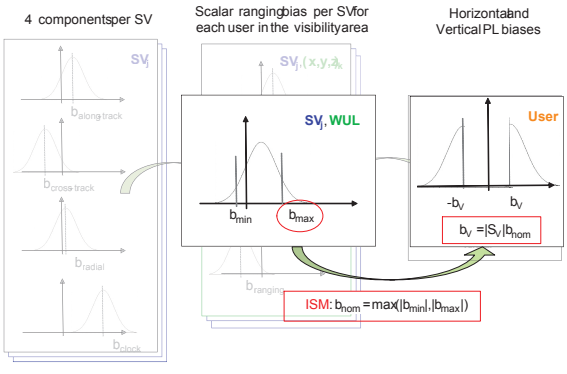


**Fig. 13** Signal In Space Error estimation in the ARAIM approach

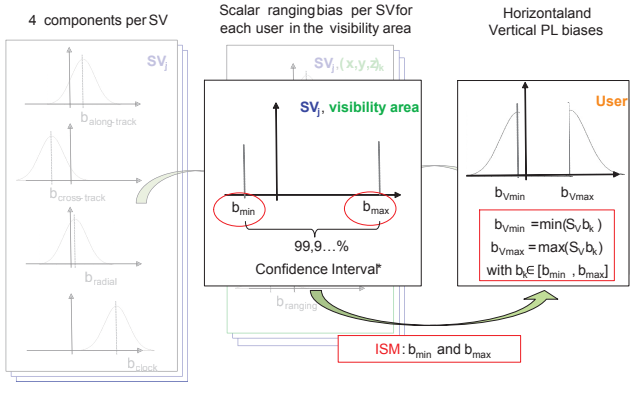


**Fig. 14** Signal In Space Error model based on two parameters approach

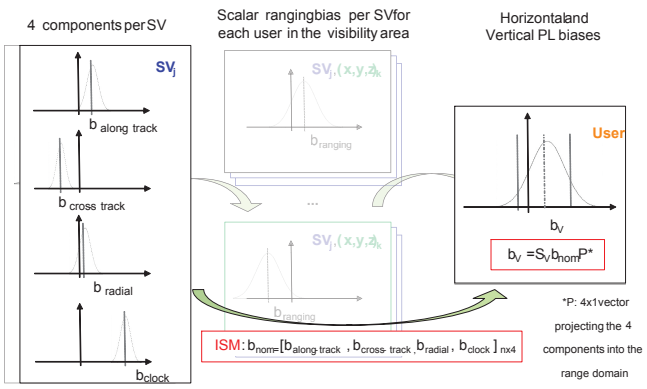


**Fig. 15** Signal In Space Error estimation in the alternative approach

carrier coherency, inter-frequency biases). In this special case of biases independent from the geometry, the 2 parameters model could already provide the best model to maximize the user performance. The 4 parameters remains the best solution for the offline ARAIM architecture.
In this novel approach the position error tails characterized with the protection levels are not anymore symmetric. The equation to be solved to estimate the protection levels described in [1], Annex on ARAIM user algorithm, eq.24 pag. 70 is the following

$$2Q\left(\frac{VPL-b_3^0}{\sigma_3^0}\right)+\sum_{k=1}^{N_{faultmode}} p_{fault,k}Q\left(\frac{VPL-T_{k,3}-b_3^k}{\sigma_3^k}\right)=P_{HMI,VERT}\left(1-\frac{P_{sat,notmonitored}P_{const,notmonitored}}{P_{HMI,VERT}+P_{HMI,HOR}}\right) \quad (13)$$

where

- $Q$ is the tail probability of a zero mean unit normal distribution. The Q function is defined as: $Q(u)=\frac{1}{2\pi}\int\frac{e^{-\frac{t^2}{2}}}{2}dt$
- $VPL$ is the Vertical Protection Level
- $b_3^k$ is the third component of the user position bias for the $k-th$ subset
- $\sigma_3^k$ is the third component of the user position standard deviation for the $kk-th$ subset
- $P_{HMI,VERT}$ is the integrity budget for the vertical component (9.8 x 10-8)
- $P_{FA,VERT}$ is the continuity budget allocated to the vertical mode (3.9 x 10-6)
- $P_{FA,HOR}$ is the continuity budget allocated to the horizontal mode
- $P_{Sat,notmonitored}$ and $P_{const,notmonitored}$ are respectively the satellite and constellation unavailability

The protection level in the solution with 2 parameters model (Figure 14) are found solving the following equation:

$$Q\left(\frac{VPL-b_{3,min}^0}{\sigma_3^0}\right)+Q\left(\frac{VPL-b_{3,max}^0}{\sigma_3^0}\right)+\sum_{k=1}^{N_{faultmode}}\frac{p_{fault,k}}{2}Q\left(\frac{VPL-T_{k,3}-b_{3,min}^k}{\sigma_3^k}\right)+\sum_{k=1}^{N_{faultmode}}\frac{p_{fault,k}}{2}Q\left(\frac{VPL-T_{k,3}-b_{3,max}^k}{\sigma_3^k}\right)=P_{HMI,VERT}\left(1-\frac{P_{sat,notmonitored}P_{const,notmonitored}}{P_{HMI,VERT}+P_{HMI,HOR}}\right) \quad (14)$$

In the solution with 4 parameters bias model Figure 15 the equation to be solved is instead

$$Q\left(\frac{VPL-b_3^0}{\sigma_3^0}\right)+Q\left(\frac{VPL+b_3^0}{\sigma_3^0}\right)+\sum_{k=1}^{N_{faultmode}}\frac{p_{fault,k}}{2}Q\left(\frac{VPL-T_{k,3}-b_3^k}{\sigma_3^k}\right)+\sum_{k=1}^{N_{faultmode}}\frac{p_{fault,k}}{2}Q\left(\frac{VPL-T_{k,3}+b_3^k}{\sigma_3^k}\right)=P_{HMI,VERT}\left(1-\frac{P_{sat,notmonitored}P_{const,notmonitored}}{P_{HMI,VERT}+P_{HMI,HOR}}\right) \quad (15)$$

The horizontal case is based on the same approach and equations are adjusted in an analogous way.
To show the difference between the two solutions and in particular the improvement of the 4 parameters solution with respect to the 2 parameters ones, an analytical analysis and an experimentation study with GPS and Galileo true orbit and clock errors have been performed and is presented in the following section.

### 2.1 4D model of Signal In Space biases with respect to one dimensional model

This section aims to analyse the conservatism of the Worst User Location approach using real satellite orbit and clock

error data. In particular it describes and estimates the performance degradation affecting the users not positioned in the WUL which apply integrity parameters valid for the WUL users.

The difference between the error projection on the WUL and that on a generic user location depends on the user position within the visibility area and on the orientation of the error vector.

In Figure 16 the unit vector $e_{\theta,\varphi}$ identifies the LOS between the satellite's center of mass and a user located on the Earth's surface within the visibility cone. To show the conservatism of the WUL approach in particular the factor between the WUL error and each generic user a k-factor is defined as follows

$$k = \frac{|\vec{E}\hat{e_{\theta,\varphi}}|}{\max_{[\theta,\varphi]\epsilon\{[-\alpha,\alpha],[0,2\pi]\}}(|\vec{E}\hat{e_{\theta,\varphi}}|)} \tag{16}$$

$k$ represents the scaling factor between each generic error and the WUL's one. Large values, close to 1, indicate that the WUL does not differ much from the user position identified by $\beta$. Values close to zero, which are highlighted in orange in Figure 17, identify situations where the user could largely take advantage by using its specific error instead of the WUL's one.

Figure 17 shows the k factor as function of the error orientation angle, $\beta$. The orange regions indicate $\beta$ angles for which the performance degradation is significant.

In order to have an overall figure of merit, indicating the performance degradation on average worldwide and over the constellation period, an averaged k factor has been estimated. The average k factor over the visibility area and over all possible error orientations is

$$\overline{k} = \int_0^{2\pi}\left(\int_0^{2\pi}\int_{-\alpha}^{\alpha} k_{\theta,\varphi,\beta} f_{\theta,\varphi} d\theta d\varphi\right) f_\beta d\beta \tag{17}$$

Assuming an uniform distribution of the users in the visibility area, $f_{\theta,\varphi}$, and using the axial symmetry

$$\begin{aligned}\overline{k} = \int_0^{\pi}\Bigg(\int_0^{2\pi}\int_0^{\alpha} \frac{E|\cos(\beta-\theta)||\cos(\varphi)|}{\max\limits_{[\theta,\varphi]\epsilon\{[0,\alpha],[0,\pi]\}}|\vec{E}\hat{e}_{\theta,\varphi}|} \\ f_{\theta,\varphi} d\theta d\varphi\Bigg) f_\beta d\beta = \\ \int_0^{\pi} \frac{E}{\max\limits_{[\theta,\varphi]\epsilon\{[0,\alpha],[0,\pi]\}}|\vec{E}\hat{e}_{\theta,\varphi}|} \\ \left(\int_0^{2\pi}|\cos(\varphi)|\int_0^{\alpha}|\cos(\beta-\theta)| f_{\theta,\varphi} d\theta d\varphi\right) f_\beta d\beta\end{aligned} \tag{18}$$

The averaged k factor depends on the distribution of the error vector, $f_\beta$. This distribution has been estimated with

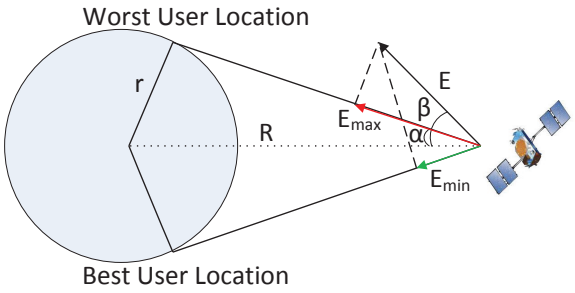


**Fig. 16** Signal In Space Error vector model with Worst User Location (WUL) and Best User Location (BUL). $R$ is the earth radius, $h$ is the satellite heigth. $\beta$ is the two dimentional angle between a line of sight and the direction from the satellite to the earth centre. $\alpha$ is the angle identifying the satellite footprint on earth.

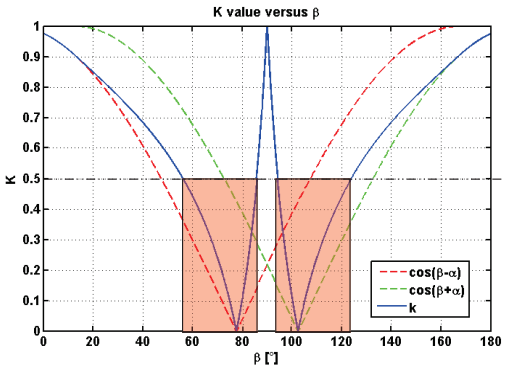


**Fig. 17** Scaling Factor as function of Signal In Space orientation angle $\beta$

real data provided by IGS for Galileo and GPS. The distributions are showed in Figure 18 and Figure 19 and they display the histogram of the satellite orbit and clock error orientation for GPS and Galileo (IGS data from 01.2003 till 04.2015 for GPS and MGEX data from 01.2013 till 04.2015 for Galileo).
Using these distributions the average k factor could be estimated. It ranges between 0.51 and 0.74 for GPS and between 0.56 and 0.72 for Galileo. This represents a significant result, in fact using the novel approach instead of the WUL'ones the URA for example could be reduced from 1m to 0.75m ensuring a significant availability improvement even with not complete constellations. [1] contains all the user availability results for several combination of bias and sigma values and several algorithm parameters. In this document the improvement, obtained when reducing URA with an inflation factor of 0.56, can be observed for several combinations of constellations and ISM parameters values.

## 3 EXPERIMENTATION RESULTS

This section describes the results of an experimentation activity performed to show the performance improvement in simulated and real scenarios. The first part describes results based on end to end simulation for multiconstellation dual frequency users. The second part describes the experimentation performed with real data collected during a flight campaign performed in March 2015.

### 3.1 Simulation Results

A dual constellation, GPS+Galileo, with dual frequency users has been simulated to show the integrity and availability improvement of the proposed solution. A 5x5 degrees usergrid worldwide has been used with the following algorithm parameters: $URA = 1m$, $URE = 2/3$, $P_{sat} = 10^{-4}$, $P_{const} = 10^{-8}$, $VAL = 35$, $HAL = 40$, masking angle 5 degrees, $P_{HMI,VERT} = 9.8 \times 10^{-8}$, $P_{FA,VERT} = 3.9 \times 10^{-6}$, $P_{FA,HOR} = 9 \times 10^{-8}$, $P_{HMI,HOR} = 2 \times 10^{-9}$;
For $b_{nom}$ a random $N_{sat} \times 1$ vector has been generated by sampling a gaussian distribution with zero mean and $50cm$ standard deviation. The value chosen is compliant with the true residual biases measured by [2], [4], [5], [10] and [11]. Figure 20 shows a short time window with the protection level time series: the classical ARAIM with one parameter bias and the proposed 4 parameters model. During the analysed period the 4 parameters solution provides smaller protection levels. In particular this result was confirmed during the whole simulation period. In fact Figure 21 shows the histogram of the difference between the two kinds of protection levels during the whole simulation and confirms that this result is always valid for each geometry condition. Beside the user availability improvement was assessed estimating the availability map for LPV-200 service, as shown

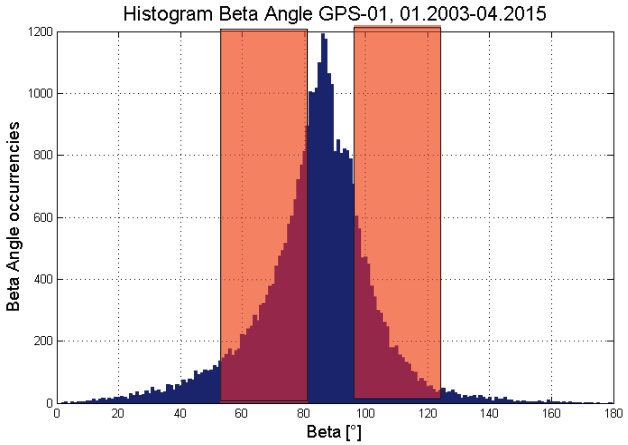


**Fig. 18** Histogram of GPS SISE as function of the vector orientation

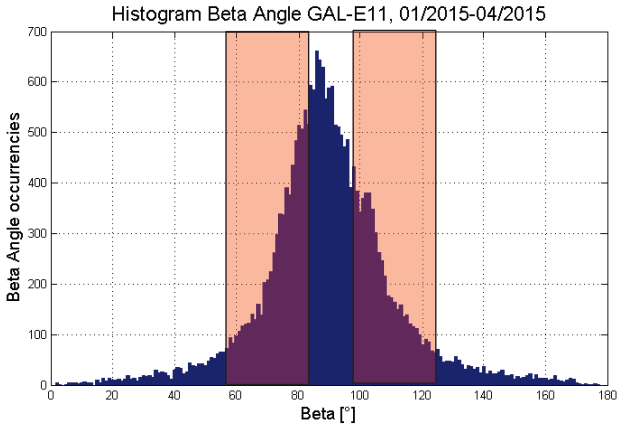


**Fig. 19** Histogram of Galileo SISE as function of the vector orientation

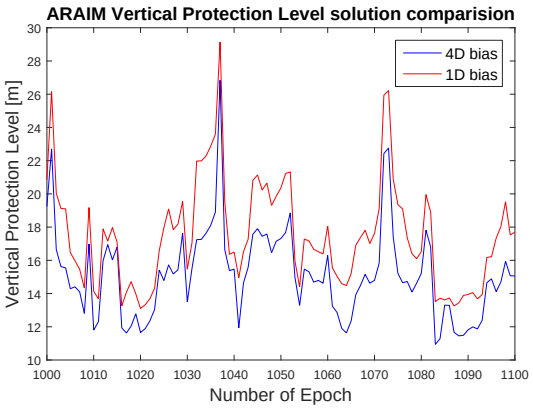


**Fig. 20** Comparison of the ARAIM Vertical Protection Level between the one parameter bias model case and the 4 parameters bias model

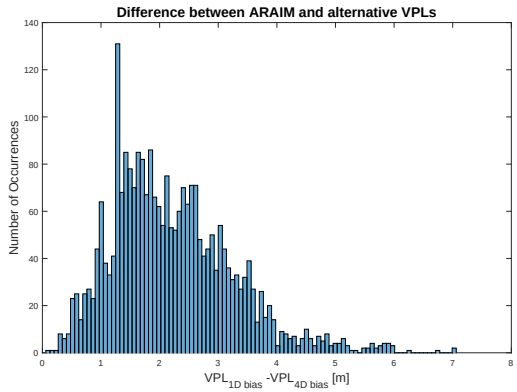


**Fig. 21** Histogram of the Vertical Protection Level difference between the ARAIM algorithms (one parameter bias model minus the 4 parameters bias model)

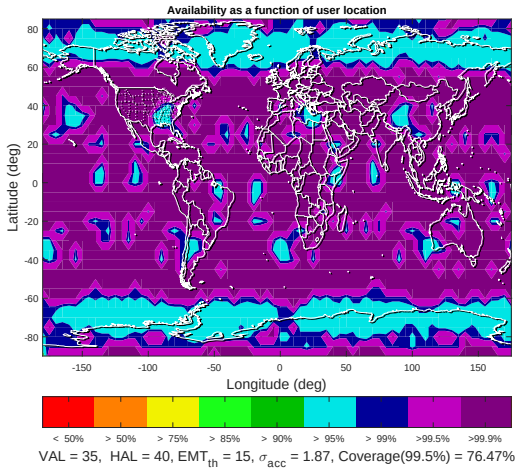


**Fig. 22** Map of the ARAIM Vertical Protection Level with one parameter bias for VAL=35

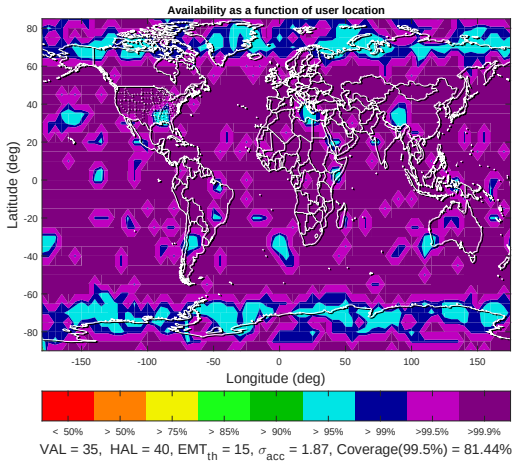


**Fig. 23** Map of the ARAIM Vertical Protection Level with 4 parameters bias for VAL=35

in Figure 22 for classical ARAIM and in Figure 23 for the proposed solution. It can be appreciated how the smaller VPLs obtained with the proposed solution provides availability improvements.

The same availability analysis was performed to assess the possibility to extend the performance further behind LPV-200. Figure 24 and Figure 25 show respectively the availability map for VAL=10m of the 1 parameter bias and that of the 4 parameters bias. It can be observed how from a completely unavailable service, the proposed approach can provide 95% availability in some regions. It is a promising result taking into account that ISM parameters used in the simulations are representative of the present constellation performance. They are conservative to cover also the early services of new constellations. This means that with smaller ISM parameters ARAIM could serve applications beyond LPV-200 (like CAT phase of flights).

### 3.2 Flight Campaign

The proposed solution and the performance improvement have been assessed also in a real environment during a flight campaign performed by the German Aerospace Center (DLR).

In March 2015, a number of flights were conducted in Braunschweig, Germany with the DLRs Dornier DO-228 26 and 27, a twin-propeller aircraft. The plane was equipped with a Javad Delta G3TH receiver. During the March campaign the new GPS IIF and Galileo signals were collected. The flight schedule was chosen during times of good visibility of GPS Block IIF and Galileo satellites. During the flight campaign, 8 Block IIF GPS and 3 Galileo satellites were available and healthy. Dual-frequency code and carrier-phase measurements on L1 (E1) and L5 (E5a) were recorded and used for the processing.

Figure 26 shows the aircraft and the location of the GNSS antenna [13]. The ISM parameter values used during the flight were the same used in the simulation scenario and specified in the previous section. The aircraft reference position was estimated in postprocessing using RTK. The user positioning was performed as specified in [8] with a smoothing time of 100s and a smoothing threshold of 10m on the code minus carrier measurements.

Figure 28 shows the time series of the Vertical Position Error [m] (green), the Vertical Protection Level [m] of the classic ARAIM using 1 parameter bias (red) and the Vertical Protection Level [m] of the 4 parameters ISM (blue). Also in this case the proposed solution provides a reduced protection level, as it is shown also by the histogram of the protection level difference in Figure 29. Besides it was important to verify that the protection level still properly bounded the position error during the whole flight campaign. It must be pointed out that this flight campaign provided first results confirming the expectation but many aspects raised which need further investigations. In particular the vertical position error resulted to be larger than

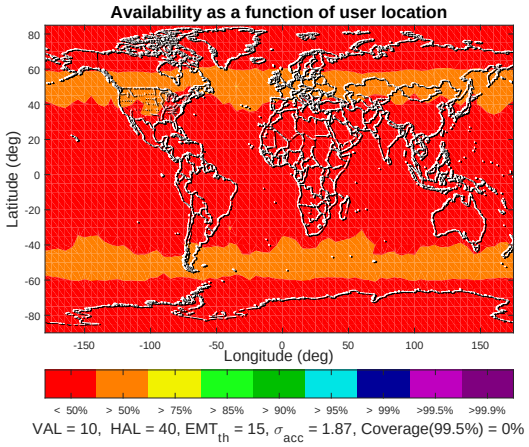


**Fig. 24** Map of the ARAIM Vertical Protection Level with 4 parameters bias for VAL=10

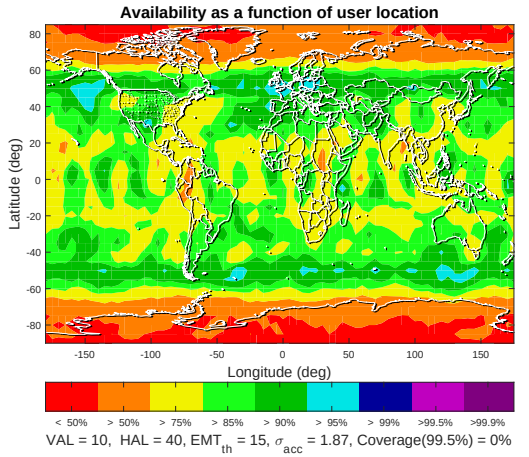


**Fig. 25** Map of the ARAIM Vertical Protection Level with 4 parameters bias for VAL=10

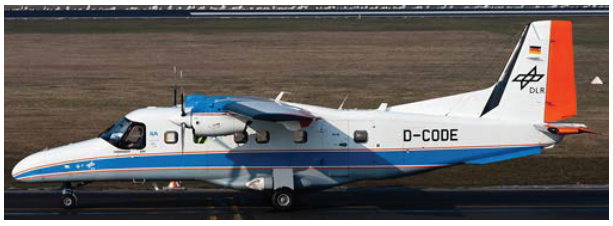


**Fig. 26** DLR's Dornier-228 research aircraft "D-CODE".

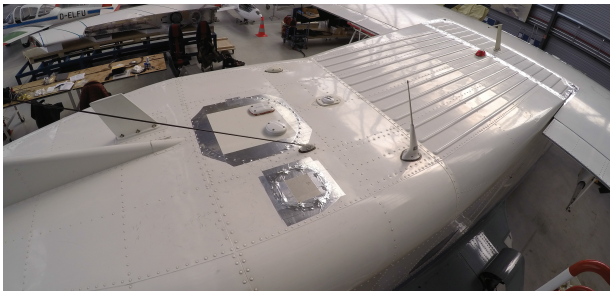

**Fig. 27** Location of the experimental GNSS antenna on the DLR's Dornier-228.

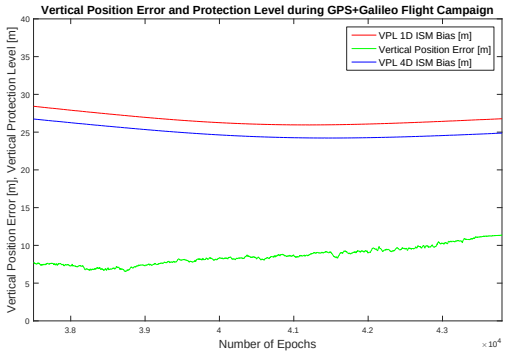


**Fig. 28** GPS+Galileo Flight Campaign Results showing the performance of the classical ARAIM with respect to the proposed approach' one. The figure shows the time series of the vertical position errors and the vertical protection levels.

expected. Possible reasons for that, which are still under investigation, are related to the aircraft multipath which was also assessed using GBAS corrections, to the presence of a repeater close to the landing strip and/or to a unexpected degraded performance of the multifrequency antenna. Other aspects which are under investigation are the inter-frequency biases L1-L5 especially of GPS IIF and Galileo satellites which might have contributed to the ranging error and beeing amplified by the smoothing algorithm. The scenario can be considered representative of an anomaly situation and was useful to verify and confirm that the proposed approach provides protection levels which safely protect the users and improves its service availability.

## CONCLUSION

Current ARAIM algorithms [1], [6], [7] treat Signal In Space biases with a conservative approach, assuming that their signs are unknown. They are bounded by the absolute value of their maximum and the worst case projection into the position domain is used to estimate the protection levels. This approach can cause situations where PLs biases are different from zero although the actually vertical user position errors are unbiased. Examples of this effect occur in case of biases common to all the satellite of one constellation or in case of ranging biases affecting only one position error component. The consequence for the user is a degradation of the availability.
Removing the common bias is a solution which addresses only partially the problem without completely solving it, as illustrated in the paper. The assumption that biases signs are unknown is based on the variation of the signs in the visibility area and with the receiver characteristics. The signs of the biases components can be estimated in the ARAIM ground monitoring or using high gain antenna facility. The paper assumes to use this information and to introduce it in the ISM. The solution presented in the paper proposes to include more parameters (in particular the four along-track, cross-track, radial and clock components instead of a single scalar value) in the ISM to model these SIS biases. This allows to provide the user with the information on the bias signs.
With this approach, the worst case projection in the user PL equations is removed and the biases reflect closely the true biases: PL biases are different from zero only when the corresponding position error is different from zero and there is no need to conservatively inflate them.
An experimentation activity with simulated data and in a real environment during a GPS+Galileo L1-L5 flight campaign assessed the real performance improvements. The results confirmed the expectations and showed the possibility to extend the use of ARAIM techniques beyond LPV-200.

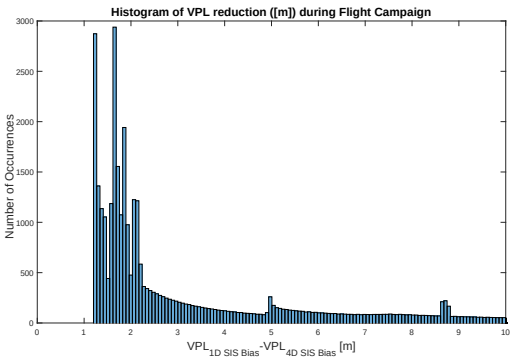


**Fig. 29** Vertical Protection Level reduction ([m]) with the proposed approach with respect to the classic ARAIM ISM model obtained during the GPS+Galileo Flight Campaign.

## REFERENCES


[1] Bilateral EU-US ARAIM Technical Sub Group of the Working Group C. GPS-Galileo Working Group C ARAIM Technical Subgroup Milestone III Report 2016, Tech. rep. Bilateral EU-US ARAIM Technical Sub Group of the Working Group C, 2013 (In pubblication process)

[2] Hauschild, A., Montenbruck, O., "The Effect of Correlator and Front-End Design on Pseudorange Biases for Geodetic Receivers", Proceedings of ION GNSS+ 2015 Conference, Tampa, Florida, September 2015, pp. 2835-2844.

[3] Wong, G., "Impact of Nominal Signal Deformations on Satellite Navigation Systems" Stanford University Ph.D. Thesis, 2014.

[4] Montenbruck, O., Hauschild, A., Steigenberger, P., and Langley, R. B., "Threes the Challenge" GPS World, July, 2010.

[5] Haines, B., Yoaz B.-S., Bertiger, W., Desai, S., and Weiss, J., "New GRACEBased Estimates of the GPS Satellite Antenna Phase- and Group-Delay Variations", 2010 International GNSS Service (IGS) Workshop, Newcastle upon Tyne, England, 28 June to July 2010.

[6] Blanch, J., Lee, Y., Walter, T., Enge, P., Pervan, B., Belabbas, B., Spletter, A., Rippl, M., "Advanced RAIM User Algorithm Description: Integrity Support Message Processing, Fault Detection, Exclusion, and Protection Level Calculation", Proceedings of the 25th International Technical Meeting of the Satellite Division of The Institute of Navigation (ION GNSS 2012), Nashville, September 2012.

[7] Joerger, M., Pervan, B., "Solution Separation and Chi-Squared ARAIM for Fault Detection and Exclusion",

Proceedings of IEEE/ION PLANS 2014, Monterey, CA, 9 May 2014, pp. 294-307.

[8] "RTCA/DO-229D: WAAS Minimum Operational Performance Specification (MOPS)", 1991.

[9] Martini, I., Rippl, M., Meurer, M. "Advanced RAIM Architecture Design and User Algorithm Performance in a real GPS, Glonass and Galileo scenario", Proceedings of ION GNSS 2013 Conference, Nashville, Tennessee

[10] Thoelert, S., et al., "GNSS Nominal Signal Distortions Estimation, Validation and Impact on Receiver Performance", ION GNSS 2015 Conference, Tampa, Florida

[11] Thoelert, S. et al., "Characterization of Nominal Signal Distortions and Impact on Receiver Performance for GPS (IIF) L5 and Galileo (IOV) E1 /E5a Signals", in Proceedings of ION GNSS+ 2014, Tampa, FL , U.S.A., September 2014

[12] Vergara M., "Tracking Error Modeling in Presence of Satellite Imperfections", accepted for publication in NAVIGATION, Journal of the Institute of Navigation.

[13] Circiu, M.-S., et al. "Evaluation of GPS L5, Galileo E1 and Galileo E5a Performance in Flight Trials for Multi Frequency Multi Constellation GBAS", Proceedings of ION GNSS 2015 Conference, Tampa, Florida

[14] International Civil Aviation Organization (ICAO), "Annex 10, Aeronautical Telecommunications, Volume I (Radio Navigation Aids)", 2005.

[15] FAA GEAS Panel, "Phase II of the GNSS Evolutionary Architecture Study", Feb. 2010.

[16] T. Walter and P. Enge, "Weighted RAIM for Precision Approach", in Proceedings of the ION GNSS Conference 1995, ION, 1995.

[17] "Airborne Supplemental Navigation Equipment Using the Global Positioning System (GPS)", Technical Standard Order (TSO), C-129, Dec 1992.